Landmarks detection by applying Deep networks

***Abstract*—Morphometric analysis is a general method applied to organisms and used to appreciate the covariances between the ecological factors and the organisms (shape, size, form,...) in which, landmark-based morphometry is known as one of the approaches to analyze the characteristics of organisms. Finding landmarks setting can give to biologists a comprehensive description of the organism. In this study, we propose a convolutional neural network (CNN) to predict the landmarks on beetle images. The network is designed as a pipeline of layers, it has been trained with a set of manually labeled landmarks dataset. Then, the network has been used to provide the morphometric landmarks on biological images automatically. The coordinates of predicted landmarks have been evaluated by computing their distance to the manual coordinates given by the biologists. Besides, the average of distance errors on each landmark has been also computed. The network model is implemented by Python on Lasagne framework.**

***Index Terms*—Morphometry, biological, landmarks, deep learning, convolutional neural networks**

I. Introduction

Morphometry analysis refers to measure the topography of an object, for example, its shape and its size. Biologists work with several parameters from organisms such as lengths, widths, masses, angles,... to analyze the interactions between environment and organisms development. Besides the traditional information, landmarks (or points of interest in the image) are known as one of the characteristics to analyze the shape. Instead of collecting all information, the shape is determined by a finite set of points, called landmarks. Landmarks store important information about the shape of the object, *for example*, the corners of the human mouth are a kind of landmarks. Currently, the landmarks are along the outline of the object but in some special cases, it could be defined inside the object. In our study, the morphometric landmarks are specific points defined by biologists. They are used in many biological studyings. But unfortunately, manual landmarks setting is time-consuming and difficult to reproduce when the operators change. Therefore, a method that gives automatic location of landmarks could have a lot of interest.

This work introduces a method for this automatic detection of the landmarks on biological images. The main idea consists on design and train of a CNN [1] with a set of manual landmarks. By this way, the trained network will learn to detect the morphometry landmarks. The dataset includes 293 beetles images from Brittany lands. All the images are presented in RGB color with two dimensions. For each beetle, the biologists took images of five parts: *left and right mandibles, head, body, and pronotum*. For each image, a set of landmarks has been manually determined by experts. In another work [2], a method has been presented to determine the landmarks on left and right mandibles (Fig. 1a). This method is based on the image processing techniques [3], combining with principal component analysis [4] and SIFT descriptor [5]. The next step has been to work with the prontoum images (Fig. 1b). For each pronotum image, a set of 8 manual landmarks have been set by the biologists. The coordinates of manual landmarks were used as the input to train the network. During the first stage, a number of 260 images and their manual landmarks were used to train and validate the network. The remaining images were used to evaluate the output model of the network in the second stage.

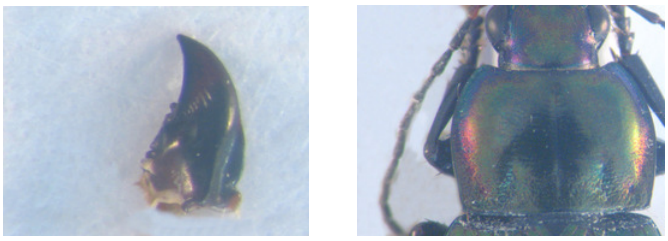

(a) Right mandible (b) Pronotum

Fig. 1: An example of right mandible and pronotum image

In the next section, we present related works to determine the landmarks on 2D images by CNN. In section 3, we present an overview about CNN. The architecture of the model, its parameters, the implementation, the experiments, and the results are presented in Section 4. At Section 5, we give the conclusion on the proposed model.

II. Related works

A landmark is a specific point that may contain useful information. For example, the tip of the nose or the corners of the mouth are landmarks on human face [6]. In image processing, we can consider two kinds of cases: the object of interest can be segmented or not. Setting landmarks can not be achieved in the same way depending on which situation we are. When segmentation can be applied, Lowe et al. [5] have proposed SIFT method to find the corresponding keypoints between two images. Palaniswamy et al. [7] have proposed a method based on probabilistic Hough Transform to automatically locate the landmarks in digital images of Drosophila wings. Krahenbuhl et al. [2] have proposed a method which have been extended from Palaniswamy's method, to determine landmarks on mandibles of beetles. The mandibles of beetle have the simple shape and easy to segment. We have obtained good enough results about determining the landmarks automatically on mandibles. Unfortunately, after several tests, we have had to conclude that this way does not provide good results with

the pronotum images because the pronotum segmentation has too many noises.

In recent years, deep learning is known as a solution in computer vision, especially for image analysis. Using CNN to determine the landmarks on 2D images has achieved better results even if the images that can not segment. Yi Sun et al. [6] have proposed cascaded CNNs to predict the facial points of interest on the human face. Zhanpeng Zhang et al. [8] proposed a *Tasks-Constrained Deep Convolutional Network* to optimize facial landmarks detection. Their model determines the facial landmarks with a set of related tasks such as head pose estimation, gender classification, age estimation, face recognition, or facial attribute inference. Cintas et al. [9] has introduced a network to predict the landmarks on human ears. After training, the network has the ability to predict 45 landmarks on human ears. In this way, we have applied CNN computing to work with pronotum landmarks.

III. Convolutional neural networks

Deep learning allows computational model composed of multiple processing layers to learn representations of data with multiple levels of abstraction [10]. Each layer extracts the representation of the input data from the previous layer and computes a new representation for the next layer. In the hierarchy of a model, higher layers of representation enlarge aspects of the input that is important for discrimination and suppress irrelevant variations. Each level of representations is corresponding to the different level of abstraction. During training, it uses gradient descent optimization method to update the learnable parameters via backpropagation. The development of deep learning opens promise results for well-known problems artificial intelligence on high dimensional data, therefore applicable to many domains: image recognition and classification [11]–[13], speech recognition [14]–[16], question answering [17], language translation [18] [19], and recognition [20][21].

A CNN consists of a number of connected layers. The layers of a CNN has neurons arranged in three dimensions: *width, height, and depth* with learnable parameters. Fig. 2 shows a classical example of CNN. It is a pipeline of usual layers: convolutional layers (CONV), pooling layers (POOLING), dropout layers (DROPOUT), and full-connected layers (FC).

A *convolutional* layer computes a dot product between its weights and a small region in the input. At the output, the results of connected local regions are combined. Convolution layer uses a set of learnable filters as parameters. Each filter is small spatially but extends the depth of the input. *Pooling* layer is used to down-sampling the input, to reduce the computational cost in remaining layers, and to control overfit. *Dropout* layer refers to dropping out units in the network. Dropping a unit out means temporarily removing it from the network, along with all its incoming and outgoing connections. *Full connected* layer refers to the output of the network. The number of outputs of the last full-connected layer are corresponding to the number of predicted values.

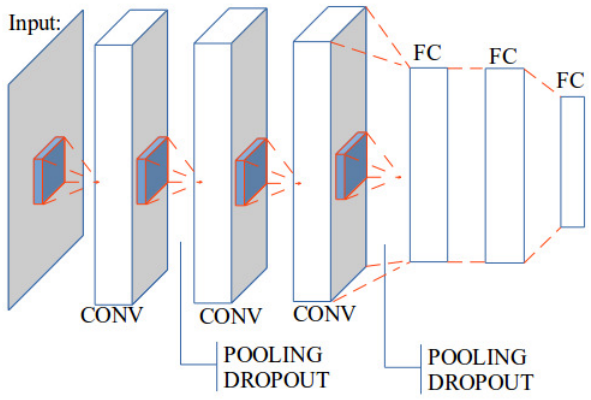

Fig. 2: An example of usual convolutional neural network

From the beginning of deep learning until now, many deep learning frameworks have been developed. Almost frameworks are open source. According to the written programming languages, the frameworks can be separated into two main groups: C++, *such as Caffe, Deeplearning4j, Microsoft Cognitive Toolkit* and Python *i.e Keras, Theano, PyTorch*. Another framework exists using more confidential languages as *Lua*.

Theano [22] is an open source framework developed by the machine learning group at the University of $Montréal$. It is a Python library that allows to define, to optimize and to evaluate mathematical expressions relating multi-dimensional arrays efficiently by using a Numpy package. Theano supports compilation on either CPU or GPU architectures. Lasagne [23] is a lightweight library in Theano. It allows to build and to train the neural networks. In this work, we have used Lasagne to implement the proposed neural network. Recently, Theano has been stopped to develop but its community is still large. The networks which have been designed by Theano are still useful and efficient in deep learning area.

IV. Application to landmarks identification

In previous sections, we have had an overview of the landmarks and CNN. In this section, we describe the designing processes of the model. We also present the process to en-large dataset, training and evaluating the model.

A. Preprocessing data

The images come from a collection of 293 beetles from Brittany lands. All the images are taken with the same camera under same conditions with a 3264×2448 resolutions. For each specific part, a set of manual landmarks has been determined by biologists. The provided dataset contains 293 images, each image with 8 landmarks provided by biologists. The dataset was split into a training set with 260 images (training and validation) and a testing set of 33 images. During the training, the network learned the information through a pair of *image and manual landmarks* in the training set. At the testing stage, the image without landmarks is given to the trained network and the predicted landmarks coordinates will be given as

output. Fig. 3 shows an example of pronotum image with its manual landmarks.

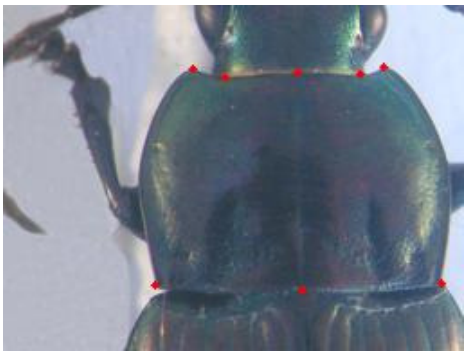

Fig. 3: An example of pronotum with manual landmarks in red points

In some published networks [11][6][9], the maximum size of the inputs is not over 256 pixels. In our case, the resolution of the image is large, it becomes a difficulty for the computing. During training and testing, the images are down-sampling to a new resolution of 256×192. Obviously, the landmark coordinates of the image are also scaled to suit their new resolution.

The proposed network has a large number of learnable parameters. In addition, the size of the dataset is limited, this means that overfitting will occur during the training process. Therefore, we need to enlarge the size of the dataset. In image processing, we usually apply transform procedure (i.e rotation, translation,...) to generate a new image but the analysis of image by CNN is most often translation and rotation invariant. Therefore, we have applied two another procedures to increase the number of images in the dataset.

The first procedure has been applied to change the value of each channel in the original image. According to this, a constant is added to a channel of RGB image and for each time, we just change the value of one of three channels. For example, from an original RGB image, if we add a constant $c = 10$ to the red channel, we will obtain a new image with a different profile histogram. By this way, we can generate three new RGB images from one RGB image.

The second procedure splits the channels of RGB images. It means that we separate the channels of RGB into three gray-scale images. At the end, we can generate six versions of original image, the total number of images used to train and validate is $260 \times 7 = 1820$ images (six versions and original image). The dataset that has been used for training and validation is split randomly by a ratio (training: 60%, validation: 40%) that has been set during the network setup.

In practical, when we work with CNN, convergence is usually faster if the average of each input variable over the training set is close to zero. Moreover, when the input is set closed with zero, it will be more suitable with the sigmoid activation function [24]. According to [24], the brightness of the image is normalized to $[0, 1]$, instead of $[0, 255]$ and the coordinates of the landmarks are normalized to $[-1, 1]$, instead of $[0, 256]$ and $[0, 192]$ before to be giving to the network.

B. Network architecture and training

Three different networks models have been proposed and trained to perform the best architecture for automatically landmarking predictions. They receive the same input of $1 \times 256 \times 192$ to train but they have different number of layers. In this section, we introduce the architectures of the networks and the process to improve the architecture from the beginning of designing.

Fig. 4 shows the architecture of the first model which is a very classical one. The network consists on three repeated-structure of a convolutional layer followed by a maximum pooling layer. The depth of convolutional layers increases from $32, 64$, and 128 with different sizes of the filter kernel: 3×3, 2×2, and 2×2. All the kernels of pooling layers have the same size of 2×2. The kernel sizes are classical as the literature. At the end, three full connected layers have been added to the network. The outputs of the full connected layers are $500, 500$, and 16, respectively. The output of the last full-connected layer corresponds to 8 landmarks (x and y coordinates) which we would like to predict. The training result shows that the architecture of this model provides overfitting and so is not good enough to solve the problem.

The second network has the same architecture as the first one. But, number of outputs at full-connected layers have been modified from 500 to 1000 to prevent the overfitting, but the result did not lead to better performances.

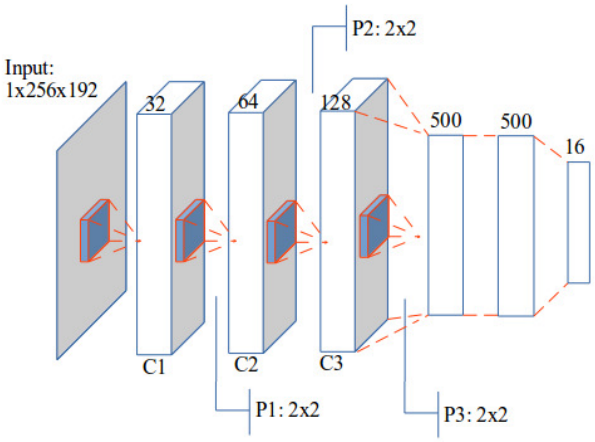

Fig. 4: The architecture of the first network

In the third network, instead of changing the parameters, we have added 4 dropout layers to the network. This is considered as the good solution to prevent the overfitting. The idea of dropout is to randomly drop units from the neural network during training. It prevents units from co-adapting too much. During training, dropout samples are done from an exponential number of different "thinned" network. At test times, it is easy to approximate the effect of averaging the prediction of all thinned networks by simply using a single

unthinned network with smaller weights. This significantly reduces overfitting and gives major improvements over other regularization methods [25]. Fig.5 shows the architecture of the third network. The first three dropout layers are supplemented to the repeated-structures followed the maximum pooling layers. In that way, structure becomes a convolution layer with square filter, followed by a *maximum* pooling and dropout layer. The probability values used for dropout layers are 0.1, 0.2, and 0.3. Actually, we keep the same value for the parameters of the convolutional $(32, 64,$ and $128)$, pooling $(3\times3,\ 2\times2,$ and $2\times2)$ and full-connected layers $(1000, 1000,$ and $16)$ as the second one.

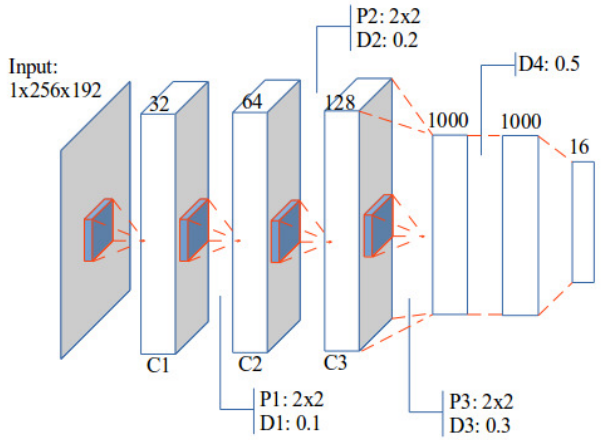

Fig. 5: The architecture of the last network

The remaining dropout layer is inserted between the first two full connected layers. The probability value of this layer is set to 0.5. The output layer still contains 16 units corresponding to the coordinates of 8 predicted landmarks.

Additionally, the network is designed with a small sharing learning rate and a momentum. As usual, these parameters have been used to perform gradient descent during backward phase to update the parameters of the layers. The value of learning rate and momentum are updated over training time to fit with the remaining number of iterations. The implementation of this architecture used Python on Lasagne framework [23] which allows to train the network on GPU. The training process took around 3 hours using NVIDIA TITAN X cards. The design of the network is available on GitHub[1].

C. Results

For the test, we have used the manual landmarks coordinates as ground truth to evaluate these ones of predicted landmarks. In the context of deep learning, landmark prediction can be seen as a regression problem. Therefore, to evaluate the results, we have used root mean square error (RMSE) to compute the accuracy of the implemented architecture.

Fig.6 and 7 show the training errors and the validation errors of a training time on the first and the third model, respectively. The blue curves present RMSE on training dataset, the green curves present the validation errors. Clearly, the overfitting has appeared in the first model. In Fig.6, we can see that if the training is able to decrease with the number of epochs[2], it is not the case of validation loss. At the opposite in the third model, we can see some different values for the two losses at the beginning but after several epochs, these values become more proximate and the overfitting problem has been solved.

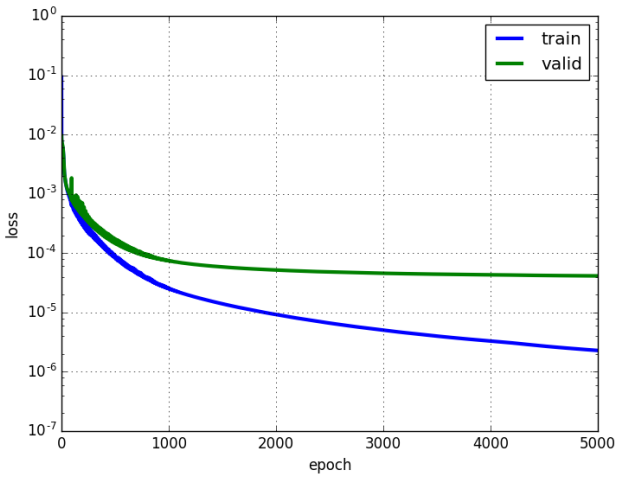

Fig. 6: Learning curves of the first model.

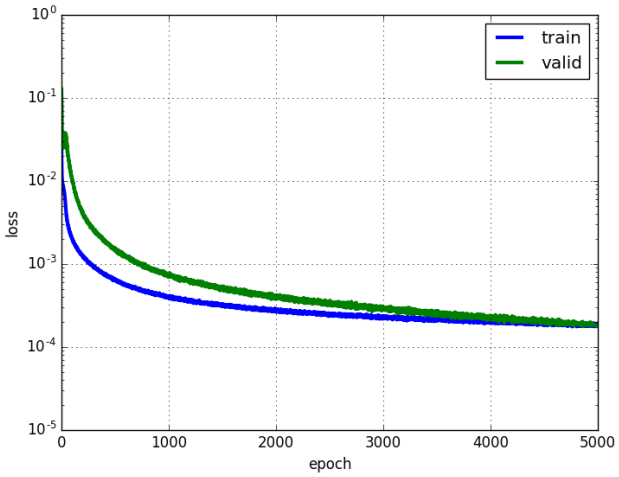

Fig. 7: Learning curves of the last model.

Fig.8 shows the predicted landmarks on test images set by the third model. Fig.8a presents a test image with the well-predicted landmarks, while Fig.8b presents the result in a bad case.

[1]It is freely obtained by request the authors.

[2]An epoch is a single pass through the full training set.

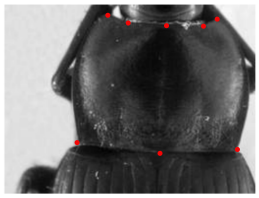

(a) Image with well-predicted landmarks

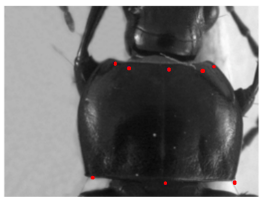

(b) Image with inaccuracy landmarks

Fig. 8: The predicted landmarks on an image in test set (red points)

For all images can compute the distance from predicted landmarks to manual landmarks. Table.I shows the average error distance given on each landmark.

TABLE I: The average distance per landmark

#**Landmark**	**Distance** (in pixels)
1	4.002
2	4.4831
3	4.2959
4	4.3865
5	4.2925
6	5.3631
7	4.636
8	4.9363

The standard deviation [26] is used to quantify the dispersion of a set of distances, for example, Fig.9 shows the distribution of the distances on the first landmark of all images. The accuracy based on the distance in each image can be separated into three spaces: the images have the distance less than average value (4 pixels): **56.66**%; the images have the distance from average value to 10 pixels (average distance plus standard deviation): **40.27**%; and the images have the distance greater than 10 pixels: **3.07**%.

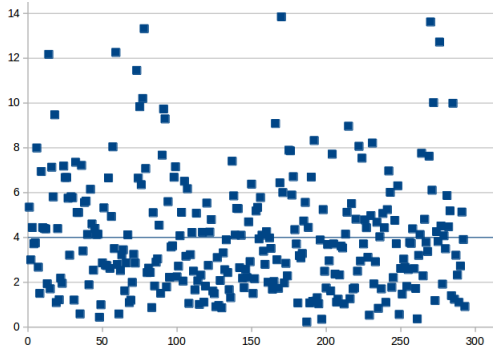

Fig. 9: The distribution of the distances on the first landmark. The blue line is the average value of all distances.

Fig.10 shows the proportion of acceptable landmarks, i.e a predicted landmark is acceptable if the distance between it and the corresponding manual one is less than the average distance plus the standard deviation value. Most of the landmarks have been detected with an accuracy greater than 75%.

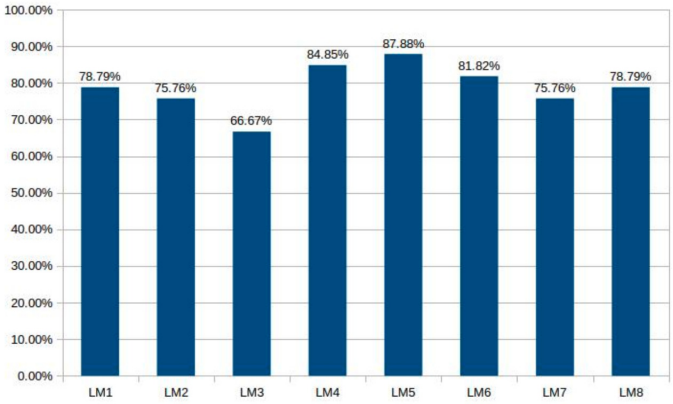

Fig. 10: The proportion of acceptable predicted landmarks

To have a comparison with the related works, we have calculated the same quality metrics for regression problems as Cintas et al. [9], i.e, coefficient of determination (r^2), explained variance (EV), and Pearson correlation, (using *scikit-learn* [27]). The best possible scores of all metrics are 1.0, lower values are worse. Table.II shows this comparison.

TABLE II: The performance of the last architecture network on regression quality metrics, comparing with the results of Cintas et al. [9]

Metric	$\mathbf{r^2}$	**EV**	**Pearson**
Cintast et al. [9]	0.884	0.951	0.976
Proposed architecture	**0.9952**	**0.9951**	**0.9974**

At the test stage, the trained network is used to predict the landmarks on a set of test images. The program outputs the predicted-landmarks of the images as TPS files; in additional, it also fills and displays the predicted-landmarks on sixteenth firstly images of test data. With the outputs are TPS files, the user can use MAELab [2] framework[3] to display the landmarks on the images.

V. Conclusion and Future Works

In the context of collaboration with biologists, the project towards replacing the manual landmarks task by automatic ones on beetle's pronotum images. The pronotum images are difficult to segment, so methods which are not supposed to be based on segmentation are necessary. In this paper, after testing several models, we have presented a convolutional neural network for automatic detection landmarks on this case. It includes three times repeated structure which consists of a convolutional layer, a max pooling layer, and a dropout layer, followed by the connected layers. During the training stage, suitable techniques are used to prevent overfitting, a common issue of the neural networks. The network was trained several

[3]MAELab is a free software written in C++. It can be directly and freely obtained by request at the authors.

times in different selections of training data. After training with the manual landmarks given by the biologist, the network is able to predict the landmarks on the set of unseen images.

In our case, the training dataset is limited. So, we have applied some techniques to en-large the dataset. The results from the test set have been evaluated by calculating the distance between manual landmarks and corresponding predicted-landmarks. The average of distance errors on each landmark has been also considered. Additional, a statistic on acceptable predicted landmarks has been computed with an accuracy greater than 75%. Using the convolutional network to predict the landmarks on biological images has promising good results in the case that the image can not be segmented. The quality of prediction allows using automatic landmarking to replace manual landmarks.

As a result, the accuracy of the network is acceptable. However, when we expect more about the accuracy of predicted landmarks (coordinates of predicted landmarks), the result of this work is still needed to improve (for example using a larger training dataset). Therefore, future research in landmarking identification appears as an improved of the worth exploring.

ACKNOWLEDGMENT

The research has been supported by DevMAP project - INRA[4]. We would like to thank my colleague, ALEXIA Marie, who has provided manual landmarks on beetle images.

REFERENCES

[1] Y. LeCun, K. Kavukcuoglu, and C. Farabet, "Convolutional networks and applications in vision," in *Circuits and Systems (ISCAS), Proceedings of 2010 IEEE International Symposium on*. IEEE, 2010, pp. 253–256.

[2] V. L. LE, M. BEURTON-AIMAR, A. KRÄHENBÜHL, and N. PARISEY, "MAELab: a framework to automatize landmark estimation," in *WSCG 2017*, Plzen, Czech Republic, May 2017. [Online]. Available: https://hal.archives-ouvertes.fr/hal-01571440

[3] J. Canny, "A computational approach to edge detection," *IEEE Transactions on pattern analysis and machine intelligence*, no. 6, pp. 679–698, 1986.

[4] J. Shlens, "A tutorial on principal component analysis," *arXiv preprint arXiv:1404.1100*, 2014.

[5] D. G. Lowe, "Distinctive image features from scale-invariant keypoints," *International journal of computer vision*, vol. 60, no. 2, pp. 91–110, 2004.

[6] Y. Sun, X. Wang, and X. Tang, "Deep convolutional network cascade for facial point detection," in *Proceedings of the IEEE conference on computer vision and pattern recognition*, 2013, pp. 3476–3483.

[7] S. Palaniswamy, N. A. Thacker, and C. P. Klingenberg, "Automatic identification of landmarks in digital images," *IET Computer Vision*, vol. 4, no. 4, pp. 247–260, 2010.

[8] Z. Zhang, P. Luo, C. C. Loy, and X. Tang, "Facial landmark detection by deep multi-task learning," in *European Conference on Computer Vision*. Springer, 2014, pp. 94–108.

[9] C. e. a. Cintas, "Automatic ear detection and feature extraction using geometric morphometrics and convolutional neural networks," *IET Biometrics*, vol. 6, no. 3, pp. 211–223, 2016.

[10] Y. LeCun, Y. Bengio, and G. Hinton, "Deep learning," *Nature*, vol. 521, no. 7553, pp. 436–444, 2015.

[11] A. Krizhevsky, I. Sutskever, and G. E. Hinton, "Imagenet classification with deep convolutional neural networks," in *Advances in neural information processing systems*, 2012, pp. 1097–1105.

[12] D. Ciregan, U. Meier, and J. Schmidhuber, "Multi-column deep neural networks for image classification," in *Computer Vision and Pattern Recognition (CVPR), 2012 IEEE Conference on*. IEEE, 2012, pp. 3642–3649.

[13] C. Szegedy, W. Liu, Y. Jia, P. Sermanet, S. Reed, D. Anguelov, D. Erhan, V. Vanhoucke, and A. Rabinovich, "Going deeper with convolutions," in *Proceedings of the IEEE conference on computer vision and pattern recognition*, 2015, pp. 1–9.

[14] T. Mikolov, A. Deoras, D. Povey, L. Burget, and J. Černockỳ, "Strategies for training large scale neural network language models," in *Automatic Speech Recognition and Understanding (ASRU), 2011 IEEE Workshop on*. IEEE, 2011, pp. 196–201.

[15] G. Hinton, L. Deng, D. Yu, G. E. Dahl, A.-r. Mohamed, N. Jaitly, A. Senior, V. Vanhoucke, P. Nguyen, T. N. Sainath *et al.*, "Deep neural networks for acoustic modeling in speech recognition: The shared views of four research groups," *IEEE Signal Processing Magazine*, vol. 29, no. 6, pp. 82–97, 2012.

[16] T. N. Sainath, A.-r. Mohamed, B. Kingsbury, and B. Ramabhadran, "Deep convolutional neural networks for lvcsr," in *Acoustics, Speech and Signal Processing (ICASSP), 2013 IEEE International Conference on*. IEEE, 2013, pp. 8614–8618.

[17] A. Bordes, S. Chopra, and J. Weston, "Question answering with subgraph embeddings," *arXiv preprint arXiv:1406.3676*, 2014.

[18] I. Sutskever, O. Vinyals, and Q. V. Le, "Sequence to sequence learning with neural networks," in *Advances in neural information processing systems*, 2014, pp. 3104–3112.

[19] S. Jean, K. Cho, R. Memisevic, and Y. Bengio, "On using very large target vocabulary for neural machine translation," *arXiv preprint arXiv:1412.2007*, 2014.

[20] H. Li, Z. Lin, X. Shen, J. Brandt, and G. Hua, "A convolutional neural network cascade for face detection," in *Proceedings of the IEEE Conference on Computer Vision and Pattern Recognition*, 2015, pp. 5325–5334.

[21] J. J. Tompson, A. Jain, Y. LeCun, and C. Bregler, "Joint training of a convolutional network and a graphical model for human pose estimation," in *Advances in neural information processing systems*, 2014, pp. 1799–1807.

[22] Theano Development Team, "Theano: A Python framework for fast computation of mathematical expressions," *arXiv e-prints*, vol. abs/1605.02688, May 2016. [Online]. Available: http://arxiv.org/abs/1605.02688

[23] S. Dieleman, J. Schlter, C. Raffel, E. Olson, S. K. Snderby, D. Nouri *et al.*, "Lasagne: First release." Aug. 2015. [Online]. Available: http://dx.doi.org/10.5281/zenodo.27878

[24] Y. A. LeCun, L. Bottou, G. B. Orr, and K.-R. Müller, "Efficient backprop," in *Neural networks: Tricks of the trade*. Springer, 2012, pp. 9–48.

[25] N. Srivastava, G. E. Hinton, A. Krizhevsky, I. Sutskever, and R. Salakhutdinov, "Dropout: a simple way to prevent neural networks from overfitting." *Journal of machine learning research*, vol. 15, no. 1, pp. 1929–1958, 2014.

[26] J. M. Bland and D. G. Altman, "Statistics notes: measurement error," *Bmj*, vol. 313, no. 7059, p. 744, 1996.

[27] P. et al, "Scikit-learn: Machine learning in python," *Journal of machine learning research*, vol. 12, no. Oct, pp. 2825–2830, 2011.

[4]https://www6.rennes.inra.fr/igepp_eng/Research-teams/Demecology/Projects/INRASPEDevMAP